Breakdown of the independent electron approximation in sequential double ionization

2011 New J. Phys. 13 093008

(http://iopscience.iop.org/1367-2630/13/9/093008)

New Journal of Physics
The open-access journal for physics

Breakdown of the independent electron approximation in sequential double ionization

A N Pfeiffer[1,4], C Cirelli[1], M Smolarski[1], X Wang[2], J H Eberly[2], R Dörner[3] and U Keller[1]

[1] Physics Department, ETH Zurich, CH-8093 Zurich, Switzerland
[2] Rochester Theory Center and Department of Physics and Astronomy, University of Rochester, Rochester, NY 14627, USA
[3] Institut für Kernphysik, Johann Wolfgang Goethe Universität, Max-von-Laue-Straße 1, 60438 Frankfurt am Main, Germany
E-mail: apfeiff@phys.ethz.ch

New Journal of Physics **13** (2011) 093008 (9pp)
Received 3 May 2011
Published 6 September 2011
Online at http://www.njp.org/
doi:10.1088/1367-2630/13/9/093008

Abstract. Correlated electron emission in strong field double ionization is dominated by recollision of the first ionized electron with its parent ion. With laser pulses that are close-to-circularly polarized, recollision may be greatly modified or avoided and the electrons are usually assumed to be field ionized without mutual interaction. Here, we present coincidence momentum measurements of the doubly charged ion and the two electrons, which are in disagreement with the independent electron assumption for close-to-circularly polarized fields. These experiments demonstrate that recollision is not the only mechanism that can lead to correlated electron emission in strong field double ionization.

In strong field double ionization, the standard picture typically distinguishes between sequential double ionization (SDI), where the electrons are assumed to tunnel-ionize independently, and non-sequential double ionization (NSDI), where the electrons cannot be treated separately [1]. Over the last few years, the research focus has been on double ionization by linearly polarized laser pulses with the result that over a wide intensity range the dominating NSDI mechanism is electron impact ionization or excitation at recollision of the first ionized electron with the parent ion, whereas at higher intensities SDI becomes dominant. The first experimental clue to

[4] Author to whom any correspondence should be addressed.

such distinguishable mechanisms was the 'knee-structure' in the ionization rate as a function of intensity [2]. Ion momentum [1] and electron correlation measurements [3] then revealed more direct evidence for the existence of recollision-induced ionization.

At this point, there remains the following open question: to what extent do mechanisms other than recollision occur which are based on electron correlation? Elliptical (close-to-circular) polarization is thought to prevent recollision in many situations and is therefore ideally suited for answering this question. Shake-up excitation of a two-electron system in intense laser fields has been measured [4], and there has been speculation about collective tunnelling [5] or inelastic tunnelling [6]. To date, quantum calculations simulating double ionization by elliptically polarized fields exceed the capability of current computers [7]. However, approaches to high-field ionization problems via classical ensembles have recently predicted NSDI behaviour for elliptically polarized laser pulses [8, 9]. Experimental investigations on circular polarization, in contrast, are rare. An exception is [10], where the structure of the momentum distribution of the double charged ions can be explained both analytically and intuitively as arising from SDI [8, 10].

In our previous work [11], we measured the ionization times in double ionization by close-to-circularly polarized laser pulses. We have found that the time of the first ionization step is in good agreement with SDI, but the second ionization step occurs earlier than predicted. Here, we present further experimental evidence that the standard picture of SDI is limited in describing double ionization by elliptically polarized laser pulses. The electron correlation spectrum generated by coincidence momentum measurements shows subtle deviations from the SDI prediction. Furthermore, two different observables are extracted, revealing an intensity dependence that is qualitatively different from the prediction of the standard SDI model. The first observable is the ratio of the number of electrons that are emitted into opposite directions to the number of electrons that are emitted into the same directions, a ratio expected to be unity on the basis of the standard independent-tunnelling SDI scenario. In contrast, we observe substantial oscillations around unity. The second observable is the variance of the ion momentum distribution along the small polarization axis. This quantity is closely related to the first observable and shows the same oscillations. This behaviour is qualitatively in agreement with a classical ensemble calculation [12].

We performed experiments with two different laser pulses: a 33 fs laser pulse at a central wavelength of 788 nm and a 7 fs laser pulse from a two-stage filament compressor [13] at a central wavelength of 740 nm. The intensity of the 33 fs pulse was adjusted by a rotating half-wave plate followed by a polarizer, and that of the 7 fs pulse was adjusted by a motorized iris. The measured ratio of Ar^{++} to Ar^{+} ions was used for intensity calibration. The total measurements consist of multiple datasets, each recorded over about 10 h. The intensity was varied continuously every 10 min between zero and the maximum intensity. The long-term stability of the laser intensity was monitored by two independent methods: firstly, by a synchronous measurement of the reflected power from a glass window, and secondly, by the ion count rate.

A Cold Target Recoil Ion Momentum Spectroscopy (COLTRIMS) apparatus [14, 15] measures the momentum of one ion and one electron in coincidence. For the following analysis, we restrict the data to events where one Ar^{++} ion and one electron are detected. The second electron is then calculated according to momentum conservation [16]. The advantage of this two-particle-coincidence method is that the detection efficiency is much more homogeneous compared to the three-particle-coincidence method where both electrons are measured. The

disadvantage is the higher portion of false coincidences, which is the detection of electron–ion pairs that do not originate from the same atom. To minimize the contribution of false coincidences, the overall probability of ionization in the laser focus needs to be as low as possible. For this measurement, we have a maximum ion count rate of 15% per laser shot at 3 PW cm^{-2}. The most reliable estimate of false coincidences can be obtained from the momentum sum of the single ionization events: for events where one Ar^+ ion and one electron are detected, the momentum sum of those two particles cancels out in the case of a true coincidence. For this measurement the portion of false coincidences varies in intensity from 19% at 1 PW cm^{-2} to 27% at 3 PW cm^{-2}, estimated from the momentum sum of the single ionization events.

An achromatic half-wave plate and a quarter-wave plate were used to adjust the polarization of the laser pulse. The ellipticity and angular orientation of the polarization ellipse were determined with a rotating polarizer. The ellipticity was 0.78 for the 7 fs pulse and 0.77 for the 33 fs pulse. The major axis of the polarization ellipse was aligned along the x-axis of our reference frame, which is the direction of the gas jet in the COLTRIMS apparatus. The momentum resolution in this direction is rather poor, about 3 atomic units (au). The minor axis of the polarization ellipse was aligned with the time-of-flight (TOF) axis of the COLTRIMS to obtain the best momentum resolution of about 0.3 au, because this is the direction of interest for the following discussion.

For the first test of an independent electron model, we ask the following question: does the emission direction of the first ionized electron influence the direction of the second electron? In the case of recollision-induced double ionization, there is a strong tendency that both electrons are emitted into the same direction. For our intensity range the semi-classical model based on SDI, which is described later in this paper, predicts a ratio of 1 : 1 for electrons that fly into the same hemisphere (parallel emission) and electrons that fly into opposite directions (anti-parallel emission).

We restrict our discussion to the coordinate along the minor axis of the polarization ellipse. Figure 1 shows the electron correlation spectrum, integrated over the scanned intensity range. The counts in the first and third quadrants represent parallel electron emission; the counts in the second and fourth quadrants represent anti-parallel electron emission. The shape of distribution in the quadrants for parallel emission deviates slightly from the distribution in the quadrants for anti-parallel emission for the coincidence data shown in figure 1(a). This is in contrast to the prediction of the standard SDI model, which predicts equally shaped islands in each quadrant. To verify that these subtle differences are not caused by calibration errors of our spectrometer, we generated non-coincidence data by pairing ions and electrons from different laser shots (figure 1(b)). The non-coincidence data indeed do not exhibit slight deviations in the different quadrants, but they show instead equally shaped islands just as the SDI model has predicted.

The statistics of our dataset is insufficient for generating two-dimensional (2D) spectra at discrete intensities, but it is possible to extract the total number of counts in the individual quadrants and display the ratio of counts as a function of laser intensity. This ratio of counts for parallel to- anti-parallel electron emission is given in figure 2 (top) for a 7 and a 33 fs pulse. We observe intensity-dependent oscillations of this ratio, especially for the 7 fs pulse and for low intensities, where the double ionization yield is very low.

To further confirm these unexpected results, we applied an additional analysis based only on ion detection that can give insights into the electron emission correlation and avoids systematic errors that might arise from biased electron detection efficiency. Figure 3 depicts the doubly charged ion momentum distribution in the plane perpendicular to the laser propagation

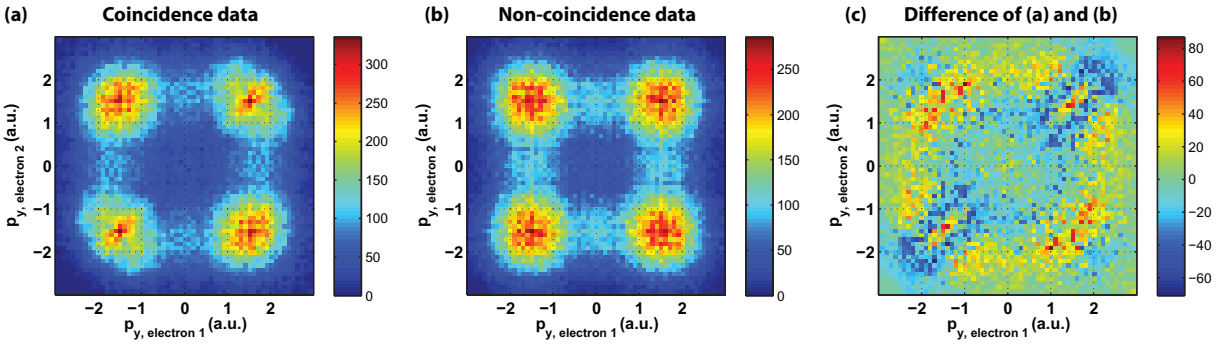

Figure 1. Momentum correlation between both electrons for double ionization of argon by a 7 fs close-to-circular polarized laser pulse. The spectrum is integrated over the intensity range of the experiment (0–3 PW cm^{-2}). The horizontal axis: momentum component of one electron along the minor axis of the polarization ellipse; the vertical axis: the same momentum component of the second electron. (a) Coincidence data: for each laser shot where the detected particles consist of one Ar^{++} ion and one electron, the momentum of the other electron is calculated according to momentum conservation. Since there is no information on whether the detected electron is the first or the second electron, both possibilities are considered and the spectrum is symmetric. (b) Non-coincidence data: the same as panel (a), but the momentum of the Ar^{++} ion is paired with the electron momentum from the successive laser shots where the detected particles consist of one Ar^{++} ion and one electron. (c) For each pixel, the number of counts in panel (b) is subtracted from the number of counts in panel (a) to highlight the subtle differences in the quadrants.

direction. Along the minor axis of the polarization ellipse (y-axis), a peak structure shows up, whereas the distribution along the major axis is close to Gaussian. This anisotropy is not caused by the different resolutions along the jet direction and TOF direction of the COLTRIMS mentioned in the description of the experimental procedure above, because the peak structure disappears when the polarization ellipse is rotated by 90°. See [8] for a detailed theoretical analysis, but the origin of the peak structure can intuitively be understood from figure 4. From momentum conservation it follows that the momentum of the doubly charged ion is equal to the negative vector sum of the two-electron momenta. Ionization occurs preferentially when the electric field vector points along the major polarization axis (x-axis), leading to an electron momentum pointing along the y-axis after acceleration by the electric field of the laser pulse [18]. Anti-parallel electron emission causes the ion to stay at close to zero momentum (central peak), whereas parallel electron emission results in the side peaks of the momentum distribution. (These are the well-known 'Z' and 'NZ' peaks of classical NSDI analysis [19].). Therefore the side-peak to central-peak ratio of counts in the $p_{y,\mathrm{ion}}$ (y-coordinate of the ion momentum) spectrum can give insights into the correlation of electron emission. For a precise estimate of the side-peak to central-peak ratio of counts, one would have to anticipate a threshold value for $p_{y,\mathrm{ion}}$ that separates the central peak from the side peaks. We avoid this source of possible errors by investigating the variance of $p_{y,\mathrm{ion}}$ instead. The variance is sensitive to the side-peak to central-peak ratio without the need for any threshold value.

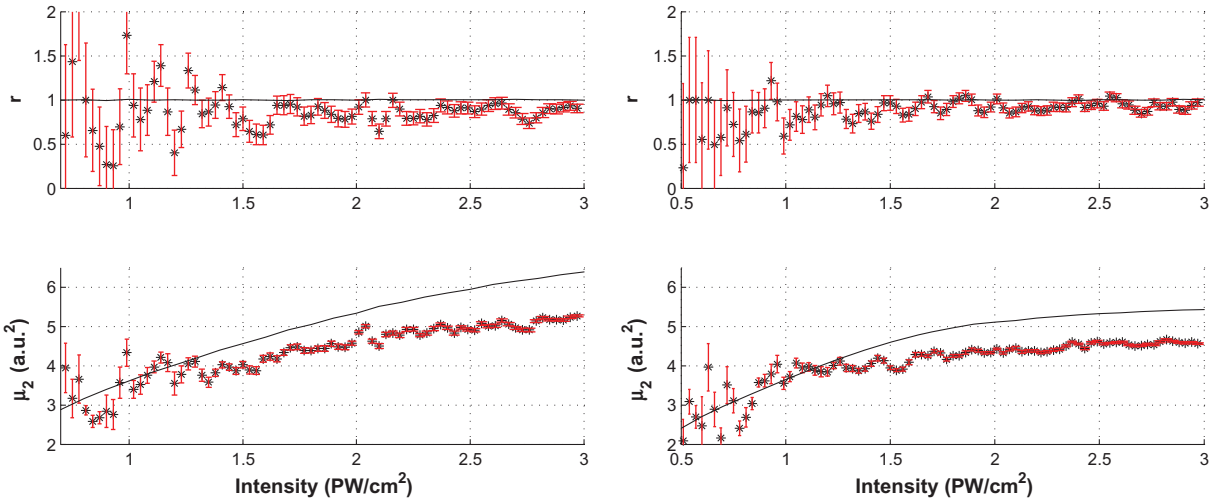

Figure 2. Two different observables as a function of intensity for a 7 fs laser pulse (left) and a 33 fs laser pulse (right). The top shows the ratio r of parallel-to-anti-parallel electron emission,

$$r = \frac{N_\mathrm{p}}{N_\mathrm{a}},$$

where N_p is the number of counts for parallel electron emission (the number of counts in the first and the third quadrant of figure 1(a), and N_a is the number of counts for anti-parallel electron emission (the number of counts in the second and the fourth quadrant of figure 1(a)). The influence of false coincidences is accounted for by subtracting the expected number of false coincidences at a given intensity, assuming that the false coincidences are equally distributed over the quadrants of figure 1 (this correction has only a very small influence on the curves). The error bars σ_r are calculated by applying Poisson statistics and standard error propagation:

$$\left(\frac{\sigma_r}{r}\right)^2 = \left(\frac{\sqrt{N_\mathrm{p}}}{N_\mathrm{p}}\right)^2 + \left(\frac{\sqrt{N_\mathrm{a}}}{N_\mathrm{a}}\right)^2.$$

The bottom shows the variance μ_2 (also called the second central moment) of the ion momentum distribution in the y-direction (the minor polarization axis). The error bars $\sigma_{\mu 2}$ are calculated as

$$\sigma_{\mu_2} = \sqrt{\frac{\mu_4 - \mu_2^2}{N}},$$

where μ_4 is the fourth central moment and N is the sample size [17]. The solid line shows the prediction of the independent electron model in both plots.

Figure 2 shows that this quantity exhibits similar oscillatory behaviour to the oscillations found in the electron correlation spectra. The oscillations found in the two observables do not give redundant information. One can think of different possible reasons for the oscillations that are observed in the variance of $p_{y,\mathrm{ion}}$. The oscillatory behaviour of the electron emission direction

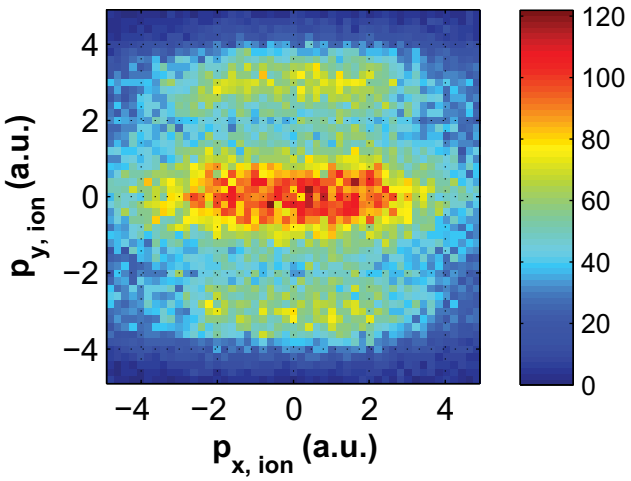

Figure 3. Momentum distribution of the doubly charged argon ions in the plane perpendicular to the laser propagation direction for a 7 fs laser pulse. The major polarization axis is oriented along the x-axis. The spectrum is integrated over the intensity range of the experiment (0–3 PW cm^{-2}).

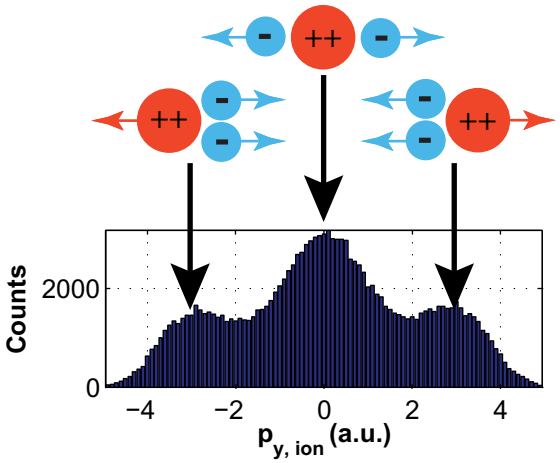

Figure 4. The distribution of the doubly charged argon ions along the minor polarization axis. The histogram is the projection of the 2D distribution depicted in figure 3 onto the y-axis. The cartoon illustrates the connection between the ion momentum distribution and the emission direction of the two electrons: the central peak corresponds to anti-parallel electron emission; the side peaks correspond to parallel electron emission. The spectrum is integrated over the intensity range of the experiment (0–3 PW cm^{-2}).

is only one possible reason and might not be the only mechanism that contributes. However, the similarity of the two oscillations suggests that the two effects are closely related.

For a quantitative illumination of these observations, we compare our results with an SDI simulation. In the calculation, we create an ensemble of ionization times for the first

and second ionization steps. The ionization times for the first and second ionization steps are chosen independently of each other according to a quasi-static ionization rate for Ar and Ar^+, respectively. For the rate, we used the formula proposed in [20], valid in both the tunnelling and the over-the-barrier ionization regime. When the electric field strength approaches the over-the-barrier value, ionization occurs at a rate high enough for saturation to become important. This is accounted for by weighting the ionization rate with the survival probability [10]. After ionization, the electron is assumed to be released into the continuum with zero kinetic energy and subsequently accelerated by the laser field. We averaged over all possible carrier-envelope-offset (CEO) phases [21], because the CEO phase was not stabilized in the experiment. Details of the simulation are given in [11]. As can be seen in figure 2, the standard SDI model reproduces the trend of the variance of p_y reasonably well. The variance increases with higher intensity because the emitted electrons acquire more momentum. However, the experimentally observed oscillations on top of this trend are not captured.

There are different ways in which the SDI simulation described above can be modified in order to account for dynamics that arise after the first ionization step. After the first ionization step, the remaining ion can exhibit an electron hole in its valence shell [22]. This state is described by a coherent superposition of the fine structure states, such that a coherent electron process is started after the first ionization step. The wavepacket evolution of the electron hole in Ar^+ influences the ionization rate for the second ionization step through the dependence of the rate on the magnetic quantum number. We incorporated this assumption about post-tunnelling dynamics into our simulation (see [11] for details), and we found that the ratio of parallel to anti-parallel electron emission is not influenced by that.

A very different result is obtained from classical ensemble calculations. These simulations are fully classical, meaning that the concept of tunnelling for the ionization step is avoided. Instead the electrons are treated fully classically from the beginning by using microcanonical initial conditions matched to the actual ionization potentials, as detailed in [23]. The process of ionization is calculated by solving the time-dependent Newton equations for all the involved particles in the presence of the electric field of the laser pulse. These classical ensemble simulations do not make the single active electron assumption of standard SDI theory, because they include all electron interactions (with each other, with the nucleus and with the laser field) at all times, both before as well as after the times of ionization of the first and second electrons. In [12], the same type of oscillation is found in the simulation that is observed experimentally in this work.

In conclusion, we have found unexpected deviations from the independent electron assumption in strong field double ionization by close-to-circularly polarized laser pulses. Two different observables of coincidence momentum data exhibit an intensity dependence that is not captured by the standard independent-electron SDI model. By carefully analysing the emission direction of the electrons it was found that the ratio of parallel to anti-parallel electron emission exhibits oscillatory behaviour around the value one at certain intensities. Similar oscillations were found by analysing the variance of the doubly charged argon ions in the direction of the minor polarization axis, avoiding any potential systematic errors in electron detection. This behaviour can be qualitatively reproduced by a classical ensemble calculation. We hope that future time-dependent Schrödinger equation simulations will shed light on the processes involved. Alternatively, the fast development of fully classical methods for elliptical polarization [9, 24] may reveal insights earlier and may provide a better understanding with a useful ‘physical picture’.

Acknowledgment

This work was supported by the NCCR Quantum Photonics, a research instrument of the Swiss National Science Foundation; by ETH research grant ETH-03 09-2; by the SNSF R'Equip grant 206021_128551/1 and by the US DOE grant ER-FG02-05ER15713. RD acknowledges support from a Koselleck Project of the Deutsche Forschungsgemeinschaft.

References

[1] Becker A, Dörner R and Moshammer R 2005 Multiple fragmentation of atoms in femtosecond laser pulses *J. Phys. B: At. Mol. Opt. Phys.* **38** S753
[2] Fittinghoff D N, Bolton P R, Chang B and Kulander K C 1992 Observation of nonsequential double ionization of Helium with optical tunneling *Phys. Rev. Lett.* **69** 2642
[3] Weber T, Giessen H, Weckenbrock M, Urbasch G, Staudte A, Spielberger L, Jagutzki O, Mergel V, Vollmer M and Dörner R 2000 Correlated electron emission in multiphoton double ionization *Nature* **405** 658
[4] Litvinyuk I V, Legare F, Dooley P W, Villeneuve D M, Corkum P B, Zanghellini J, Pegarkov A, Fabian C and Brabec T 2005 Shakeup excitation during optical tunnel ionization *Phys. Rev. Lett.* **94** 033003
[5] Eichmann U, Dörr M, Maeda H, Becker W and Sandner W 2000 Collective multielectron tunneling ionization in strong fields *Phys. Rev. Lett.* **84** 3550
[6] Kornev A S, Tulenko E B and Zon B A 2003 Kinetics of multiple ionization of rare-gas atoms in a circularly polarized laser field *Phys. Rev.* A **68** 043414
[7] Becker W and Rottke H 2008 Many-electron strong-field physics *Contemp. Phys.* **49** 199
[8] Wang X and Eberly J H 2009 Effects of elliptical polarization on strong-field short-pulse double ionization *Phys. Rev. Lett.* **103** 103007
[9] Mauger F, Chandre C and Uzer T 2010 Recollisions and correlated double ionization with circularly polarized light *Phys. Rev. Lett.* **105** 083002
[10] Maharjan C M, Alnaser A S, Tong X M, Ulrich B, Ranitovic P, Ghimire S, Chang Z, Litvinyuk I V and Cocke C L 2005 Momentum imaging of doubly charged ions of Ne and Ar in the sequential ionization region *Phys. Rev.* A **72** 041403
[11] Pfeiffer A N, Cirelli C, Smolarski M, Dörner R and Keller U 2011 Timing the release in sequential double ionization *Nat. Phys.* **7** 428
[12] Wang X and Eberly J H 2011 Multielectron effects in sequential double ionization with elliptical polarization arXiv:1102.0221v1
[13] Hauri C P, Kornelis W, Helbing F W, Heinrich A, Courairon A, Mysyrowicz A, Biegert J and Keller U 2004 Generation of intense, carrier-envelope phase-locked few-cycle laser pulses through filamentation *Appl. Phys.* B **79** 673
[14] Ullrich J, Mooshammer R, Dorn A, Dörner R, Schmidt L P H and Schmidt-Böcking H 2003 Recoil-ion and electron momentum spectroscopy: reaction-microscopes *Rep. Prog. Phys.* **66** 1463
[15] Dörner R, Mergel V, Jagutzki O, Spielberger L, Ullrich J, Moshammer R and Schmidt-Bocking H 2000 Cold target recoil ion momentum spectroscopy: a momentum microscope to view atomic collision dynamics *Phys. Rep.* **330** 95
[16] Weckenbrock M, Hattass M, Czasch A, Jagutzki O, Schmidt L, Weber T, Roskos H, Loffler T, Thomson M and Dörner R 2001 Experimental evidence for electron repulsion in multiphoton double ionization *J. Phys. B: At. Mol. Opt. Phys.* **34** L449
[17] Riley K F, Hobson M P and Bence S J 2002 *Mathematical Methods for Physics and Engineering* (Cambridge: Cambridge University Press)
[18] Smolarski M, Eckle P, Keller U and Dörner R 2010 Semiclassical model for attosecond angular streaking *Opt. Express* **18** 17640

[19] Ho P J and Eberly J H 2003 Different rescattering trajectories related to different total electron momenta in nonsequential double ionization *Opt. Express* **11** 2826
[20] Tong X M and Lin C D 2005 Empirical formula for static field ionization rates of atoms and molecules by lasers in the barrier-suppression regime *J. Phys. B: At. Mol. Opt. Phys.* **38** 2593
[21] Telle H R, Steinmeyer G, Dunlop A E, Stenger J, Sutter D H and Keller U 1999 Carrier-envelope offset phase control: a novel concept for absolute optical frequency measurement and ultrashort pulse generation *Appl. Phys.* B **69** 327
[22] Goulielmakis E *et al* 2010 Real-time observation of valence electron motion *Nature* **466** 739
[23] Ho P J, Panfili R, Haan S L and Eberly J H 2005 Nonsequential double ionization as a completely classical photoelectric effect *Phys. Rev. Lett.* **94** 093002
[24] Wang X and Eberly J H 2010 Elliptical polarization and probability of double ionization *Phys. Rev. Lett.* **105** 083001